SOILS AND FOUNDATIONS Vol. 46, No. 4, 437–448, Aug. 2006
Japanese Geotechnical Society

NONLINEAR DYNAMIC BEHAVIOR OF PILE FOUNDATIONS: EFFECTS OF SEPARATION AT THE SOIL-PILE INTERFACE

B. K. MAHESHWARI[i] and H. WATANABE[ii]

ABSTRACT

During strong ground motion, pile foundations are subjected to two special effects. First, behavior of the soil surrounding the piles is nonlinear. Second, large inertial forces are generated in the soil around the pile heads, causing separation between the soil and pile. In this paper, a new approach is presented to overcome material nonlinearity of the soil as well as geometrical nonlinearity arising due to separation. The analysis is performed in two steps. To account for material nonlinearity, equivalent linearization is used in conjunction with a hyperbolic model of the soil. The hyperbolic model defines the nonlinear stress-strain relationship of the soil. To deal with separation, a Winkler soil model is used. The dynamic stiffness reproduced by the soil model is changed according to the degree of separation. Depending on the level of excitation, different cases of separation arise which are investigated with skeleton curves. It has been found that due to separation, dynamic response of the soil-pile system increases whereas the dynamic stiffness decreases significantly.

Key words: dynamic analysis, dynamic stiffness, nonlinear response, pile foundations, separation, soil-pile interface, Winkler soil model (**IGC**: H1)

INTRODUCTION

In the broad area of pile dynamics, research is primarily focused on linear dynamic analysis. Substantial research efforts have been made on the linear analysis of single pile and pile groups in the frequency domain, as shown by many researchers such as Novak (1974), Blaney et al. (1976), Novak and Nogami (1977), Kaynia and Kausel (1982), Gazetas (1984), Dobry and Gazetas (1988) and Makris and Gazetas (1992). Few researchers performed the time domain analyses. Matlock et al. (1978) developed a unit load transfer curve approach, also known as *p-y* curves, for the time domain nonlinear analysis. Additionally based on plane strain medium assumption in the frequency domain (Novak et al., 1978), Nogami and Konagai (1986), and (1988) have developed time domain analysis methods for axial and lateral response of single piles, respectively. Their analyses are based on the assumptions of the Winkler soil model.

For a rational and safe design of structures supported on piles, it is important that supporting pile foundations are designed adequately considering the behavior of soil surrounding the piles. During strong ground motions, behavior of soil becomes nonlinear and due to large inertial forces, slippage and separation may occur at the soil-pile interface. A rational design of pile foundations should take into account the material nonlinearity of the soil as well as geometrical nonlinearity. In this paper both of these nonlinearities are introduced for the dynamic analyses of pile foundations for lateral loading. Method proposed herein has practical significance in the earthquake resistant design of pile foundations and supported structures.

During strong ground motion or dynamic excitation from the pile cap (or foundation structure), caused by machine excitations or wind induced vibration forces, large inertial forces are generated in the soil around the pile heads causing the phenomena of slippage and separation. Due to the complexity of the modeling involved, most of the existing theories, dealing with the dynamic behavior of soil-pile systems, assume perfect contact between the pile and soil. However this is not valid for such large excitations. The focus in recent years has shifted to incorporate the nonlinear behavior of soil media in the analysis. Using the finite element method in the frequency domain, Angelides and Roesset (1981) performed a nonlinear analysis. Nogami and Konagai (1987) and Nogami et al. (1992) extended their earlier developed time domain models to incorporate geometrical nonlinearity for axial and lateral response, respectively. Based on the Winkler hypothesis, El Naggar and Novak (1996) presented a nonlinear analysis for pile groups in the time domain.

Here a simple and computationally efficient approach

[i] Asst. Professor, Dept. of Earthquake Engineering, Indian Institute of Technology Roorkee, India (bkmahfeq@iitr.ernet.in) (formerly Doctorate Student, Dept. of Civil Engineering, Saitama University, Japan).
[ii] Deceased, Formerly Professor, Dept. of Civil Engineering, Saitama University, Japan.
The manuscript for this paper was received for review on July 16, 2005; approved on March 10, 2006.
Written discussions on this paper should be submitted before March 1, 2007 to the Japanese Geotechnical Society, 4-38-2, Sengoku, Bunkyo-ku, Tokyo 112-0011, Japan. Upon request the closing date may be extended one month

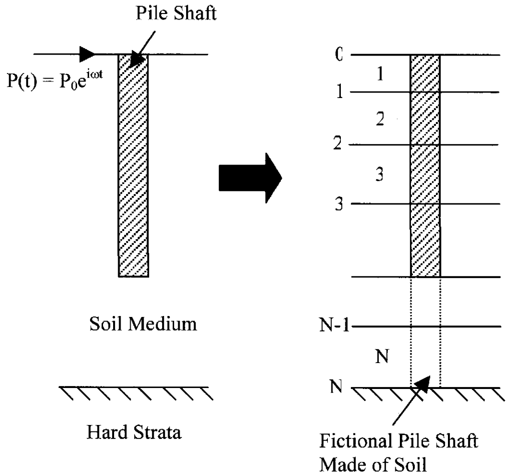

Fig. 1. Idealization of soil-pile system: division into a number of slices

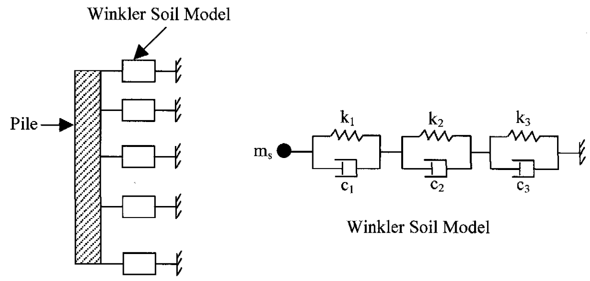

Fig. 2. Modeling soil-pile system for separation using Winkler soil model

is presented to deal with material nonlinearity of soil and separation at the soil-pile interface. When excitation is of such level that shear strains in the soil media fall in the medium range (i.e. approximately 10^{-5} to 10^{-3}) then the hyperbolic model of soil has proved to be quite promising to deal with material nonlinearity, Ishihara (1996). For such cases the shear modulus and damping ratio, both of which depend on the level of shear strain, are the key parameters to model the soil medium. In this paper, equivalent linearization in conjunction with a hyperbolic model is used to deal with material nonlinearity. Methodology is briefly described here, and further detail can be found in Maheshwari and Watanabe (1998).

Once material nonlinearity of the soil media is modeled appropriately, the existing time domain Winkler soil model is used to deal with separation. The model proposed by Nogami and Konagai (1988) is used for the linear analysis and a new method is proposed to deal with separation. The methodology presented herein is simple and computationally more efficient as it deals with separation in a rational manner.

Depending on the level of excitation, there may be a number of scenarios for separation. Three general cases are identified, skeleton curves for all these cases are derived and relevant formulation is presented. The linear and nonlinear responses and dynamic stiffness of an end-bearing single pile are compared. Using the methodology proposed, it is possible to analyze floating piles. Also the proposed methodology can be readily extended for pile groups in a similar fashion as suggested by El Naggar and Novak (1996).

MODELING OF THE SOIL-PILE SYSTEM

A model for the linear pile analysis in the time domain as proposed by Nogami and Konagai (1988) is shown in Figs. 1 and 2. It is assumed that a hard stratum exists either at the pile tip or at some finite depth below the tip. Thus, if a pile is not resting directly on the bedrock then also it can be analyzed using the same methodology as end bearing pile by assuming a fictitious pile (made of soil) exists below the pile tip. As shown in Fig. 1, the soil-pile system is divided into a number of layers. Properties of the soil media may vary from layer to layer but assumed to be constant in a particular layer. The load is assumed to act at the pile head, which may be either due to machine excitation or due to inertial forces generated during seismic excitation. In this manuscript only harmonic excitation is considered, though it is possible to consider transient excitation.

TIME-DOMAIN WINKLER SOIL MODEL FOR HORIZONTAL VIBRATION

Winkler's hypothesis is used to analyze each layer of the soil-pile system. According to this hypothesis, the soil-pile interaction force at one level is related to the displacement at that level only. Thus a separate Winkler model is used for each layer, which is uncoupled from that used in other layers. As shown in Fig. 2, each unit of Winkler soil model consists of three Voigt models and a mass connected in series. This model is developed from the frequency domain plane strain solution (Novak et al., 1978). Brief details of the development of this model, emphasizing on its physical meaning, are described below:

Consider an infinitely long vertical massless circular cylinder embedded in an infinite elastic medium and subjected to lateral harmonic excitations. Under the conditions considered, strains do not vary in the axial direction of the cylinder (and displacement w in vertical direction is zero), and thus a plane strain condition exists. The expression of the response of the cylinder is obtained by solving two wave equations of the medium involving displacements u (in radial direction) and v (in tangential direction).

The complex horizontal stiffness related to a unit length of the cylinder is given by (Novak et al., 1978):

$$S_x = \pi G(a_0^*)^2 \times \left[\frac{4K_1(b_0^*)K_1(a_0^*) + a_0^*K_1(b_0^*)K_0(a_0^*) + b_0^*K_0(b_0^*)K_1(a_0^*)}{b_0^*K_0(b_0^*)K_1(a_0^*) + a_0^*K_1(b_0^*)K_0(a_0^*) + b_0^*a_0^*K_0(b_0^*)K_0(a_0^*)}\right] \tag{1a}$$

where in the absence of material damping

$$b_0^* = \frac{a_0^*}{\eta}; \quad \eta = \sqrt{\frac{2(1-\nu)}{(1-2\nu)}} \tag{1b}$$

and

$$a_0^* = a_0 i; \quad a_0 = \omega r_0 / v_s; \quad i = \sqrt{-1} \tag{1c}$$

where a_0 = dimensionless frequency; r_0 = radius of the cylinder; v_s = shear wave velocity = $\sqrt{G/\rho}$; G = shear modulus of the medium; ρ = mass density of the medium; ω = frequency of harmonic excitation; ν = the Poisson's ratio; K_j = second kind modified Bessel function of order j;

Taking the limit $\nu \rightarrow 0.5$, $\eta = \infty$; and $b_0^* = 0$; Eq. (1a) is simplified to:

$$S_x = \pi G (a_0^*)^2 \left[\frac{4K_1(a_0^*)}{a_0^* K_0(a_0^*)} + 1 \right]$$

$$= 4\pi G a_0^* \frac{K_1(a_0^*)}{K_0(a_0^*)} + \pi G (a_0^*)^2 \tag{2a}$$

Substituting value of a_0^* in second term, this equation is simplified to

$$S_x = 2S_z - \rho \pi r_0^2 \omega^2 \tag{2b}$$

where

$$S_z = 2\pi G a_0^* \frac{K_1(a_0^*)}{K_0(a_0^*)} \tag{2c}$$

The first term in Eq. (2b), S_z is identical to that for the vertical stiffness (Novak et al., 1978) and the second term corresponds to an inertia effect of a vertical mass equal to the volume of the cylinder. It can be shown that the lateral stiffness of the medium with Poisson's ratio other than 0.5 can be approximately expressed in the same form as that in Eq. (2b) with a small modification (Nogami and Konagai, 1988) i.e.

$$S_x = \xi_k(\nu) S_z - \xi_m(\nu) \rho \pi r_0^2 \omega^2 \tag{3}$$

where functions $\xi_k(\nu)$ and $\xi_m(\nu)$ depend only on Poisson's ratio. Values of these functions are given in Table 1.

Using Eq. (3), frequency dependent complex stiffness can be expressed as a stiffness of a system made of frequency-independent springs, dashpots and mass. Thus Winkler soil model for horizontal vibration consists of three Voigt models (each consisting of a spring and a dashpot connected in parallel) and a mass connected in series as shown in Fig. 2. The model parameters are (Nogami and Konagai, 1988):

$$m_s = \xi_m(\nu) \rho \pi r_0^2 \tag{4a}$$

$$\begin{Bmatrix} k_1 \\ k_2 \\ k_3 \end{Bmatrix} = \xi_k(\nu) G \times \begin{Bmatrix} 3.518 \\ 3.581 \\ 5.529 \end{Bmatrix} \tag{4b}$$

$$\begin{Bmatrix} c_1 \\ c_2 \\ c_3 \end{Bmatrix} = \xi_k(\nu) \frac{G \times r_0}{v_s} \times \begin{Bmatrix} 113.097 \\ 25.133 \\ 9.362 \end{Bmatrix} \tag{4c}$$

Using Eq. (4), the model parameters of Winkler soil model can be found. Constant numerical values on the right side of Eqs. (4b) and (4c) are the same as that used in the Winkler soil model for vertical vibration. These values are found by best-fit curve method so that stiffness and damping of the unit (Winkler model) match those for a plane strain continuous medium given by Novak et al. (1978). Even though parameters of the model are frequency independent, the model can still reproduce the dynamic response of a plane strain medium for a wide frequency range except at very low frequencies (relative to the fundamental frequency of the soil deposit). This is a very important characteristic by virtue of which the model can be used in the time domain analysis.

Table 1. Functions $\xi_k(\nu)$ and $\xi_m(\nu)$ (after Nogami and Konagai, 1988)

Poisson's ratio (ν)	$\xi_k(\nu)$	$\xi_k(\nu)$
0.50	2.000	1.0000
0.49	1.940	0.7828
0.48	1.883	0.6420
0.47	1.831	0.5336
0.46	1.784	0.4464
0.45	1.741	0.3740
0.43	1.667	0.2628
0.40	1.580	0.1428
0.35	1.476	0.0352
0.25	1.351	0
0.20	1.311	0
0.10	1.252	0
0.00	1.213	0

Physical meaning of the model can be understood that all the three springs and dashpots (together) reproduce the stiffness and damping of the dynamic stiffness of the soil medium while the mass reproduces the inertial effects. It shall be noted that each unit of a Winkler soil model reproduces the dynamic stiffness of soil in one layer around the pile (on both sides), as shown in Fig. 2.

Using this model, complex soil stiffness of the medium for lateral vibration at a particular frequency ω is given by, as shown by Nogami et al. (1992) for the far-field element model:

$$k_u = k_s - m_s \omega^2 \tag{5a}$$

where

$$k_s = \left[\sum_{n=1}^{3} \frac{1}{(k_n + i\omega c_n)} \right]^{-1} \tag{5b}$$

Where the constants m_s, k_n and c_n are given by Eqs. (4a), (4b) and (4c), respectively.

In Fig. 3, the complex soil stiffness (computed for a steady-state harmonic motion) reproduced by the time-domain Winkler soil model is compared with those directly computed by a plane strain solution in the frequency domain (Novak et al., 1978). It can be observed that there is a good agreement between the two results for

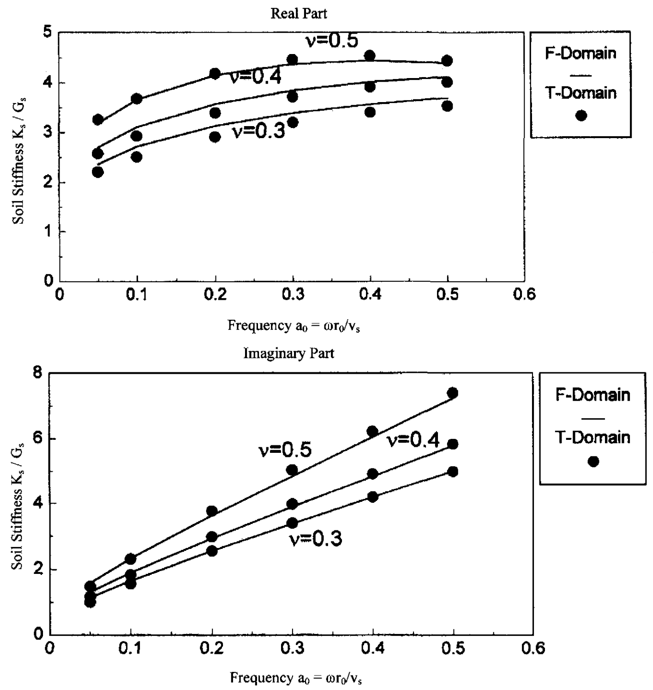

Fig. 3. Complex soil stiffness in horizontal vibration using frequency and time domain approaches

both real and imaginary parts. This validates the Winkler model for lateral vibration. Further detailed verification can be found in Maheshwari (1997).

In the proposed approach, skeleton curves for three cases of separation are derived. The dynamic stiffness reproduced by the Winkler soil model is varied according to these skeleton curves, thus simulating effects of separation. This approach is described in detail in *Possible Cases of Separation*.

FORMULATION FOR NONLINEAR ANALYSIS

The following sections describe the methodology proposed for this complex problem. *Shear Strains in Soil Media* and *Hyperbolic Model of Soil and Equivalent Linearization* briefly describe the methodology to deal with material nonlinearity, while *Governing Equation of Motion in the Time Domain* provides brief detail on the equation of motion in the time domain. In *Possible Cases of Separation*, different possible cases of separation are formulated and skeleton curves are presented and discussed in detail.

Shear Strains in Soil Media

A rigorous three-dimensional approach, based on Green's function formulation and proposed by Kaynia and Kausel (1982), is used to deal with linear pile analysis. In this approach the force-displacement relationship is expressed in terms of the degrees of freedom at the ends of the pile (pile head and pile tip). Since the external force(s) acting at pile head and the boundary condition(s) at the pile tip are known, the displacements at the pile ends can be found using the aforementioned force-displacement relationship. Subsequently the forces at the pile-soil interface P can be computed with the known pile end displacements, as shown by Maheshwari and Watanabe (1998). Once the force vector P is known, the displacement at any point in the vicinity of the pile in all the three directions can be computed using the relation:

$$U = F_s' P \tag{6}$$

where $=F_s'$ denotes the soil-flexibility matrix derived for the distance at which displacements are desired when the source of the disturbance is the axis of the pile. With the known displacements in all three directions, the shear strains for the planes perpendicular to the z axis (vertical) are computed by (Maheshwari and Watanabe, 1998):

$$\gamma_{xz} = \frac{u_2 - u_0}{\Delta z} + \frac{w_1 - w_0}{\Delta x} \tag{7a}$$

$$\gamma_{yz} = \frac{v_2 - v_0}{\Delta z} + \frac{w_3 - w_0}{\Delta y} \tag{7b}$$

where u, v and w are the displacements in the x, y and z directions, respectively, and the subscript denotes the location of points with subscript ($_0$) for the point where strains are calculated. For computation, $\Delta x = \Delta y = \Delta z = r_0$ is taken, where r_0 is equal to the radius of the pile. Out of two shear strains computed from Eqs. (7a) and (7b), the maximum one is selected. Thus the maximum shear strain in each layer of soil is found at a particular frequency. This process is repeated for all the frequencies under consideration to find the absolute maximum value of shear strain in each layer.

Hyperbolic Model of Soil and Equivalent Linearization

The shear modulus and damping ratio, both of which depend on the level of shear strain, are the key parameters to model the soil medium. Therefore to model nonlinear behavior of the soil a hyperbolic model of soil is used. The governing equations for this model are Hardin and Drnevich (1972)

$$\frac{G}{G_{max}} = \frac{1}{1 + \gamma/\gamma_r} \tag{8a}$$

$$\frac{D}{D_{max}} = \frac{\gamma/\gamma_r}{1 + \gamma/\gamma_r} \tag{8b}$$

where G and D represent the shear modulus and damping ratio (at a particular strain γ) for soil, respectively; G_{max} and D_{max} represent the maximum values of G and D, respectively; γ_r represents the reference strain for the given soil media. Using Eqs. (8a) and (8b), new properties of soil medium are found based on 2/3 of the absolute maximum value of shear strain. Thus, iterations are carried out until properties of soil get converged, Watanabe (1978).

Governing Equation of Motion in the Time Domain

The loading time history is digitized at each time increment. Governing equation of motion for the flexural response of the pile at $t = t_i$, is:

$$E_pI\frac{d^4u_i}{dz^4}+m_p\ddot{u}_i=-p_i \tag{9}$$

where u_i and $\ddot{u}_i$ are lateral displacement and acceleration of the pile respectively at the soil-pile interface at time t_i; E_pI is the bending stiffness of the pile shaft; m_p is the mass per unit length of the pile; and p_i is the soil-pile interaction force at t_i. By expressing the acceleration $\ddot{u}_i$ in terms of the displacement u_i, and the known displacement, velocity, acceleration at previous time step t_{i-1}, and expressing the interaction force p_i in terms of displacement u_i (such as shown later in Eq. (11a)) Eq. (9) is solved for response u_i of the soil-pile system. Further detail on solution technique is given in SOLUTION OF EQUATION OF MOTION AND SEISMIC ANALYSIS.

Possible Cases of Separation

As the level of the excitation (depending on the amplitude and frequency contents) increases, the force at the soil-pile interface increases. When this force exceeds a certain threshold value(s), given by the confining pressure and shear strength of the soil, separation occurs in a particular way. Although there may be a number of cases for this phenomenon but these may be classified in the following four groups:

No Separation

In this case it is assumed that pile and soil remains in perfect contact. This is expected to occur if

$$p_i \leq p_c \quad \text{where} \quad p_c=2\pi r_0\sigma_c \tag{10}$$

Where as before p_i is the soil-pile interaction force and p_c is the threshold value for the interaction force derived from the confining pressure σ_c in the soil springs. As shown by Nogami and Konagai (1988), for perfect contact, p_i (the soil-pile interaction force at time t_i,) can be expressed in terms of displacement as follows:

$$p_i=q_i+m_s\ddot{u}_i \tag{11a}$$

where

$$q_i=ku_i+d_i \tag{11b}$$

$$k=\left[\sum_{n=1}^{3} I_n(\Delta t)\right]^{-1} \tag{11c}$$

$$d_i=-k\sum_{n=1}^{3} u_{i-1,n}e^{-\delta_n\Delta t}-kp_{i-1}\sum_{n=1}^{3} H_n(\Delta t) \tag{11d}$$

$$H_n(\Delta t)=\frac{1}{k_n}\left[\frac{1}{\delta_n\Delta t}-\left(1+\frac{1}{\delta_n\Delta t}\right)e^{-\delta_n\Delta t}\right] \tag{11e}$$

$$I_n(\Delta t)=\frac{1}{k_n}\left[\left(1-\frac{1}{\delta_n\Delta t}\right)+\frac{1}{\delta_n\Delta t}e^{-\delta_n\Delta t}\right] \tag{11f}$$

$$\delta_n=k_n/c_n \tag{11g}$$

It shall be noted that k_u in Eq. (5a) represents the dynamic stiffness for Eq. (11a). However, the former is in the frequency domain while the later is in the time domain. In these equations, the constants m_s, k_n and c_n are determined using Eqs. (4a), (4b) and (4c), respectively with the converged properties of soil (obtained after equivalent linearization), while Δt represents the time step.

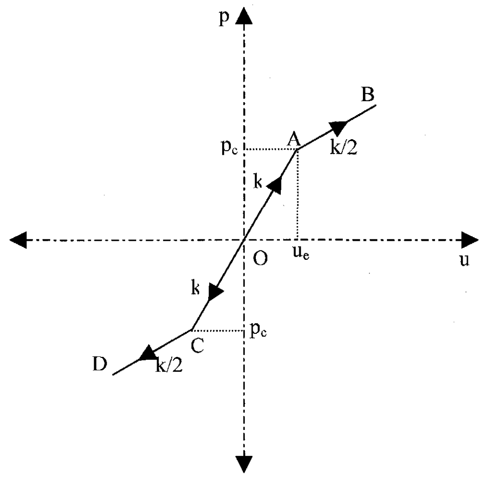

Fig. 4. Skeleton curve for separation on one face of the pile

Separation on One Face of the Pile Only

For this case, it is assumed that at a time the soil separates from one side of the pile only. In other words, at all time there is a perfect contact between the soil and pile on at least one side. This would be possible only, if the gap formed on one side (until rebound occurs from the other side) is less than the elastic displacement of the soil. This will occur if

$$p_c \leq p_i \leq p_f \quad \text{where} \quad p_f=2\pi r_0\sigma_f \tag{12}$$

where p_f is the ultimate threshold value for the interaction force derived from the compressive strength σ_f of the soil. Since the soil resistance of both sides of the pile has been modeled using a single Winkler model, when soil at one side of the pile separates, the dynamic stiffness k_u of the model, is reduced to half for further loading. The dynamic stiffness (including the effect of inertia) of the soil model in the lateral direction is given by Eq. (5). It can be seen from these equations that the dynamic stiffness will be reduced to half, if value of each element of Winkler soil model (i.e. all three springs and dashpots as well as lumped mass of soil) is reduced to half. Thus when separation occurs on one side of the pile only, Eqs. (11) are still valid provided the dynamic stiffness of the spring is reduced to half by multiplying each parameter of Winkler soil model by 50%.

The skeleton curve showing force-displacement relationship of soil spring for this case is as shown in Fig. 4. Conditions for separation and re-connection can be derived from this figure. Since it is assumed here that the force in the soil spring remains within the elastic limit, under periodic loading, the displacement is recovered during load reversal. Thus, as shown in Fig. 4, the stiffness of the soil spring remains half until reconnection between the soil and pile occurs at point A during reversal of load. After reconnection the stiffness is restored to its

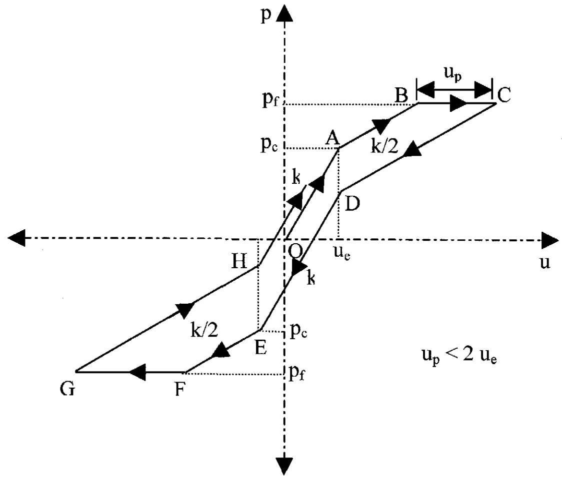

Fig. 5. Skeleton curve for separation on one face and yielding on other

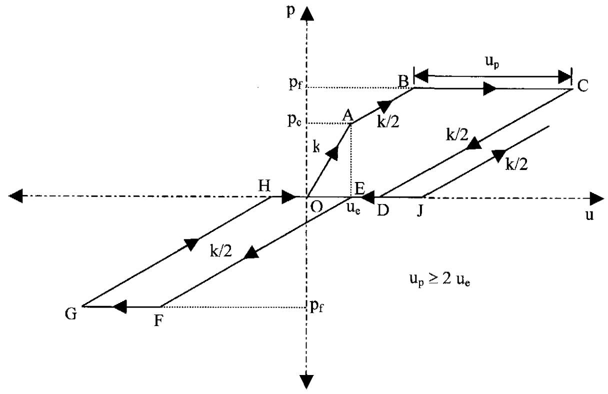

Fig. 6. Skeleton curve for separation on both faces

full value.

Again the soil is separated on other side at point C (Fig. 4), if the interaction force in the spring again reaches its threshold value. For periodic loads this cycle of separation and reconnection continues for subsequent cycles of loading.

Separation on One Face While Yielding on Another

The skeleton curve for this case is shown in Fig. 5. Here it is assumed that the soil on one side of the pile is separated (point A) and, before reversal of the load occurs, the force in the soil spring on other side reaches its ultimate limit (point B). Thus, yielding of soil occurs on the other side. Yielding occurs here but no permanent gap in the soil is considered. Displacement up to separation (point A) will be referred to as elastic displacement (u_e) and the displacement during yielding (B-C) as a plastic displacement (u_p). Before reversal of the load occurs (at point C), the interaction force reaches the yielding value (at point B). For this case plastic displacement (u_p) should be less than two times of elastic displacement (u_e). Condition for this case can be formulated as

$$p_i \geq p_f \quad \text{and} \quad u_p < 2u_e \tag{13}$$

Second condition in Eq. (13) can be derived by the geometry of the Fig. 5 for the limiting case when point D touches the u axis. During yielding, the stiffness of soil spring reduces to zero and displacement occurs at a constant value of force equal to p_f as shown in Fig. 5. During yielding the equation of motion (Eq. (9)) can be solved directly setting $p_i = p_f$, and the right hand side does not depend on u_i.

During load reversal (C-D), the stiffness of soil spring is half of the original value and at point D the pile again comes in contact with the separated part (before the force in the spring reaches a zero value). At point D the soil spring attains its full original stiffness. This process is repeated in another direction (D-E-F-G-H) in the same way as (O-A-B-C-D) and this cycle continues.

Separation on Both Faces (Delinking)

The skeleton curve for this case is shown in Fig. 6. Steps OA and AB are the same as in the previous case but it is assumed that in this case yielding (B-C) occurs for a longer duration, and the condition for this case to exist is

$$p_i \geq p_f \quad \text{and} \quad u_p \geq 2u_e \tag{14}$$

As a result of longer yielding, during rebound (C-D), the force in the spring that is not separated reaches a zero value (point D) before the pile reconnects the soil on the separated part (on another face). Since all the potential energy is released, the soil separates from the other side also. Thus, delinking of the soil and pile occurs, and the pile moves freely to another side (D-E) until it comes in contact with the soil again (point E). From point E to F there is connection on one side only and then at point F the force in the soil spring reaches the yield value again and this process continue. During delinking, the right-hand side of the equation of motion (Eq. (9)) is zero and it is solved for free movement of the pile.

In the above three cases (Separation on One Face of the Pile Only, Separation on One Face While Yielding on Another and Separation on Both Faces (Delinking)) three special terms, separation, yielding and delinking have been used to define the different phenomena occurring. The meaning of these terms in the present context are summarized in Table 2.

SOLUTION OF EQUATION OF MOTION AND SEISMIC ANALYSIS

Winkler soil model provides the dynamic stiffness of the soil and when it is coupled with dynamic stiffness of the pile it provides the dynamic stiffness of the system for a single layer. Thus governing equation of motion for the flexural response of the pile at a particular time step is given by Eq. (9) (reproduced here for convenience):

$$E_p I \frac{d^4 u_i}{dz^4} + m_p \ddot{u}_i = -p_i \tag{15}$$

where soil-pile interaction force p_i on the right hand side is defined in FORMULATION FOR NONLINEAR ANALYSIS for a particular case of separation. For

Table 2. Possible cases (considered) in separation

Phenomena	Definition	Criteria (p_i = Soil-pile interaction force)	Physical modeling (k_u = Dynamic stiffness)
No separation	Perfect contact on both faces of the pile	$p_i \leq p_c$; ($p_c = 2\pi r_0 \sigma_c$)	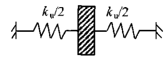
Separation	Separation at one face, perfect contact on other	$p_c \leq p_i \leq p_f$; ($p_f = 2\pi r_0 \sigma_f$)	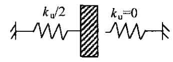
Yielding	Separation at one face, yielding of soil on other	$p_i \geq P_f$;	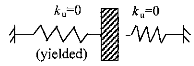
Delinking	Separation at both faces; free movement of the pile	If yielding occurs and $u_p \geq 2u_e$. (Occurs when $p_i = 0$).	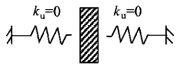

example for no separation, p_i can be expressed in terms of displacement u_i (Eq. (11)). With this Eq. (15) is simplified to a fourth order differential equation, solutions of which will provide the displacement u_i however the expression becomes extremely complex after a few time steps. In order to develop an approximate solution in a simple form, the expression for the displacement u_i is assumed to be a polynomial form with least number of terms required to define boundary conditions at the ends of the pile segment. Unknown constants of this expression are determined by satisfying boundary conditions at the ends of the segment. Thus finally a relationship between displacement (rotation) and shear force (moment) at the two ends of the segment can be obtained. Next considering the equilibrium and compatibility conditions between the two adjacent segments, for all segments, leads to the expression for the responses at the bottom of the nth segment given by (Nogami and Konagai, 1988):

$$\left(u_i,\ \theta_i,\ \frac{M_i}{E_p I},\ \frac{P_i}{E_p I}\right)_n^T = [T_n]\left(u_i,\ \theta_i,\ \frac{M_i}{E_p I},\ \frac{P_i}{E_p I}\right)_0^T + \{Q_n\} \quad (16)$$

where the subscripts 0 indicates the pile head. Computation of matrices T_n and Q_n depend on the properties and geometry of the soil-pile system, time interval Δt and known values (of displacement and rotation) at previous time step, details can be found in the above cited reference.

Seismic analysis is performed for the vertically propagating shear waves. Control point for seismic excitation (where input motion is applied) is assumed at the surface of the bedrock. For seismic analysis, shear force (and moment) acting at the bedrock ($n=N$) is known while displacement and rotation are zero at $n=N$. Thus Eq. (16) can be solved to find the displacements (including rotation) and forces (including moment) at pile head due to seismic excitation. Once these values at pile head are known, the same at any depth (n) can be found from Eq. (16).

DATA USED IN COMPUTATION AND VERIFICATION OF THE PROPOSED METHOD

The following initial properties for the soil and pile are used in computation:

$$E_p/E = 800;\quad \rho/\rho_p = 0.7;\quad \sigma_c = 100\ \text{kPa};$$
$$\sigma_f = 200\ \text{kPa};\quad L/d = 15;\quad \nu = 0.35;$$

where E_p and E are Young's modulus for the pile and soil respectively. L and d are the length and diameter of the pile, respectively, and ρ_p is mass density of the pile. The pile is assumed to be of concrete. The modulus as well as the strength of the soil mentioned are those at the surface and assumed to be linearly increasing with the depth. The values of these parameters for bottom layer are assumed to be twice of that for the top layer.

Since a rigorous method is used, its verification is imperative. One of the illustrations for verification is shown in Fig. 3 where complex soil stiffness computed by proposed method is compared with plane stain solution. It shall be noted that agreement between two methods is good and results shown can be compared with those presented by Nogami and Konagai (1988). Authors also performed experimental verification (though for linear case only) shown in the following section.

EXPERIMENTAL VERIFICATION

Small-scale tests for soil-pile system were conducted on shake table at Saitama University. Tests were carried out for a single pile as well as for a group of 5 piles for sinusoidal excitation. Objective of tests were to verify the theoretical model and algorithm used in the analysis. Tests were conducted only for linear analysis (assuming perfect bond between soil and pile). Here results of a single pile system are presented.

Model used in experiments is shown in Fig. 7. A synthetic resin i.e. acrylic material was used for the pile and for the footing. Properties of the material (simulating pile) are:

$$E_p = 3.041\ \text{GPa};\quad \rho_p = 1190\ \text{Kg/m}^3$$

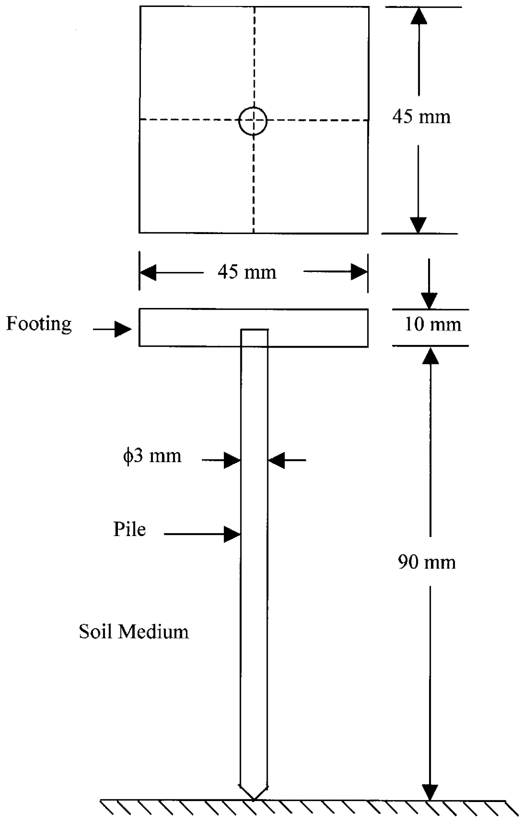

Fig. 7. Model used in experiments for a single pile

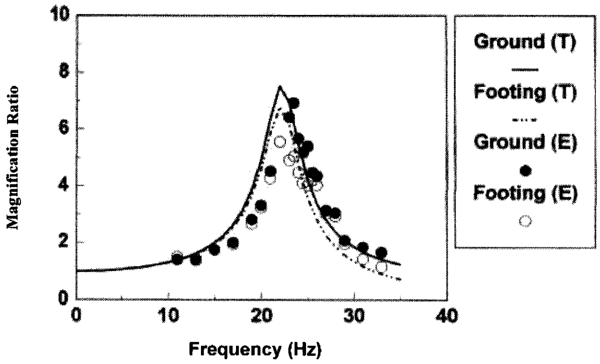

Fig. 8. Comparison of theoretical (T) and experimental (E) results

For simulation of ground, a box (dimension of which were very large as compared to footing) filled with silicon putty is taken. Properties of this material (simulating soil) are:

$$E=0.1894\ \text{MPa};\quad \rho=945\ \text{Kg/m}^3;\quad \nu=0.292$$

Authors would like to acknowledge that these properties of the material used to represent pile and soil are significantly different than those of real material. However still ratio $E_p/E=16{,}000$ is within practical range (representing a very soft soil and a very stiff pile). Further ratio $\rho/\rho_p=0.79$ is very close to that used for real materials and ν is in practical range. It shall be noted that for a soil-pile interaction analysis ratios (E_p/E and ρ/ρ_p) are more important than the absolute values of Young's modulus and density (of soil and pile) as demonstrated by other researchers.

In experiments, displacements were measured (using strain gauges) at three different levels:

(i) Input harmonic displacement (amplitude u_0) at the bottom surface of the ground (box).

(ii) The free-field displacement (amplitude u_g) at the ground surface i.e. at a considerable distance from the pile where there will be no influence of piles.

(iii) At the centroid of the footing (amplitude u_f).

Normalizing the latter two displacement amplitudes, with respect to the amplitude of input motion, corresponding magnification ratios are computed. Figure 8 shows the variation of these magnification ratios with frequency of excitation (f) in Hz. It can be observed that theoretical and experimental results are in very good agreement for both responses of ground and footing. Also it can be observed that there is not a significant difference in the response of ground and footing which is justified from the fact that for experimental range of frequency, parameter ($a_0=\omega r_0/v_s<0.04$) and for this low value of dimensionless frequency a_0, ratio (u_f/u_g) remains near unity (Kaynia and Kausel, 1982). Thus this verifies the model and algorithm used in the analysis.

EFFECTS OF NONLINEARITY

The effects of separation on the behavior of an end-bearing single pile are examined for harmonic loading using the time domain approach. The time history is plotted, and then amplitude of interaction force and displacement at the pile head are noted to infer various results. Results are presented as follows:

Depth of Separation

To estimate the depth of the separation, the variation of the maximum interaction force and the lateral displacement with depth is plotted in Fig. 9 (assuming no separation). In this figure the depth z is normalized with the length L of the pile. It can be seen that both the force and displacement have higher values around top of the pile, and decrease rapidly at greater depth. From this figure it can be seen that the soil strength is higher at greater depth while the interaction force is lower. This suggests that separation occurs only in some top layers where interaction force is exceeding the resistance of the soil.

Response for No Separation

Force and displacement time histories for top layer assuming no separation are shown in Fig. 10 for a single pile. The hysteresis loop for the force and displacement is also shown in this figure. It can be observed that for a steady-state harmonic motion, both displacement and interaction force time histories represent steady-state conditions. In addition, value of displacement amplitude obtained was verified with those obtained by frequency domain method (Kaynia and Kausel, 1982). This also

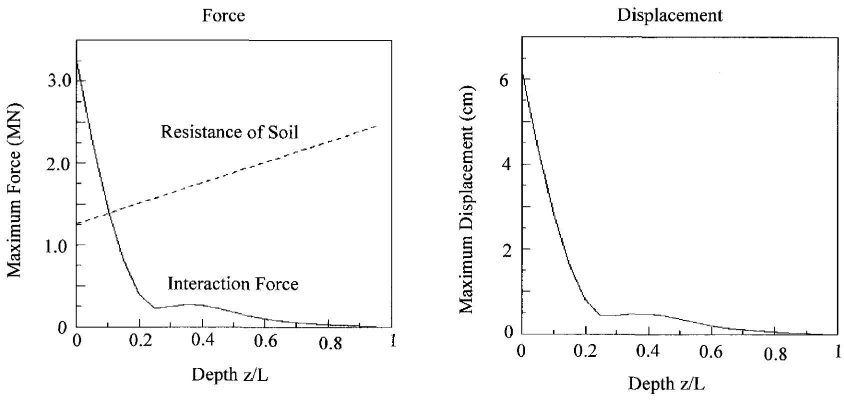

Fig. 9. Variation of maximum force and displacement at soil-pile interface with depth

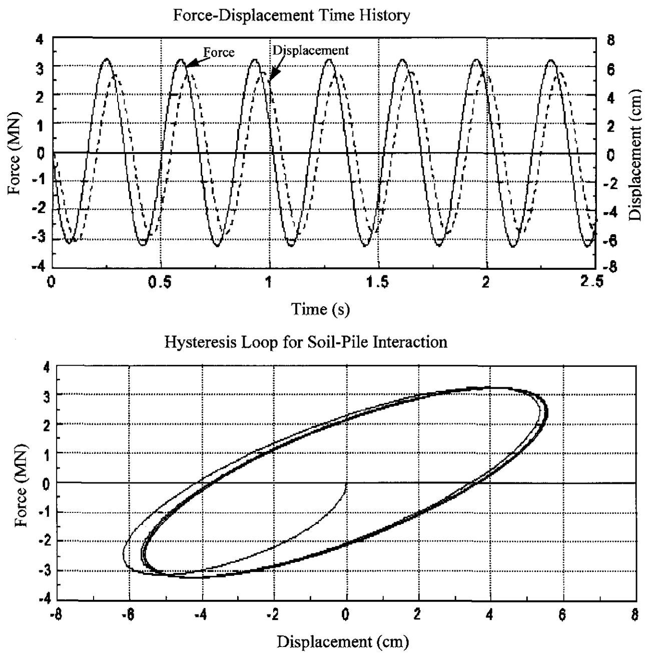

Fig. 10. Behavior of soil-pile interaction in top layer assuming no separation

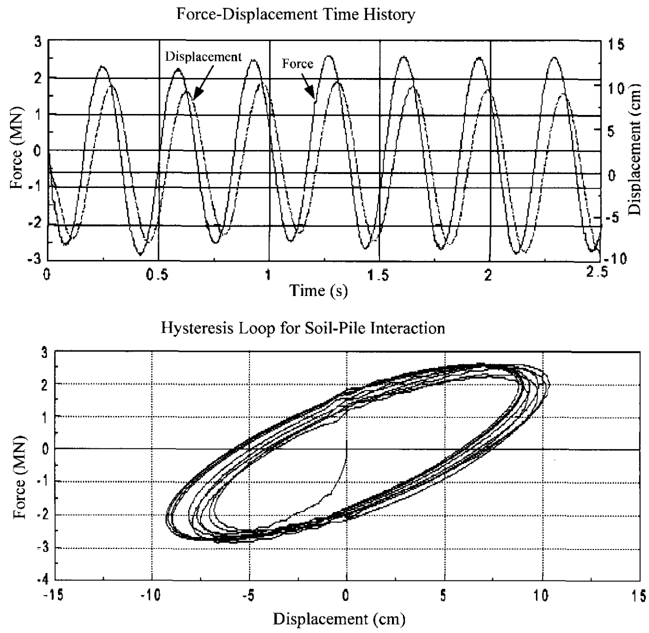

Fig. 11. Behavior of soil-pile interaction in top layer assuming separation at one face (without phase correction)

verifies the proposed method.

Concept for the Phase Correction

The force-displacement time histories for separation on one face are shown in Fig. 11. It can be observed that it does not represent a steady state condition even for an input harmonic excitation. The reason for this is investigated and described as follows.

In case there is no damping in the soil, the load and displacement will not have a time lag. Therefore the load vs. displacement can be traced correctly on the hysteresis curve. However, in the case of damping (which usually exists), the time lag disturbs recognizing the trace of true load corresponding to displacement (response) at the point of reconnection on the hysteresis curve. Thus, if the calculated load, corresponding to the displacement at the point of reconnection is adopted, this is not the true load on the hysteresis. Therefore, the time lag must be removed to know correctly where load and displacement are on the hysteresis curve. Due to this lag, the force and displacement time histories do not attain a steady state condition as shown in Fig. 11.

Since dual criteria have been used to define separation (criteria is force) and reconnection (criteria is displacement), and these two parameters have time lag, a correction was required so that displacement was only criterion for separation as well as for reconnection. Figure 12 shows the process to remove this time lag, so called phase correction. It can be seen that when there is no damping, both force and displacement reaches its maximum value simultaneously and no correction is required. But in the case of damping, a phase correction is required. The essence behind this phase correction is that after separation (defined by the value of force), reconnection should be at a time where one obtains the same force as it was at the time of separation, after accounting for the time lag as shown in Fig. 12. Thus with

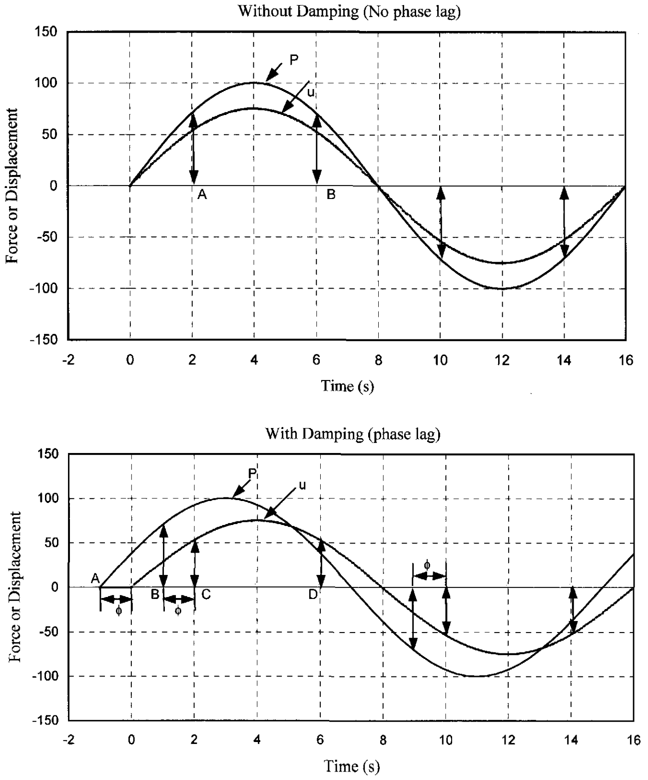

Fig. 12. Concept for the phase correction

damping, if separation occurs at point B then reconnection would be at point D as illustrated in second part of Fig. 12.

Separation on One Face

After applying the phase correction, Fig. 13 shows the force displacement relationship for the top layer. Due to phase correction, both force and displacement time histories become steady state. Comparison of Figs. 11 and 13 shows the effect of phase correction. Subsequent results are derived with phase correction.

The responses for the linear (no separation) and nonlinear (separation on one face) cases are compared in Fig. 14. As expected, separation increases the displacement and decreases the force, i.e. the nonlinearity is reducing the stiffness of the soil. It can be observed that due to effect of separation, amplitude of displacement is increased from about 5.5 cm to 8.0 cm i.e. an increase of about 45%. Similarly second half of Fig. 14 shows that due to nonlinearity, amplitude of force is reduced by about 25%.

The dynamic stiffness of a single pile-soil system is computed at different frequencies by the time domain approach presented here. The results for linear and nonlinear cases are shown in Fig. 15. The frequency is presented in dimensionless form using the radius of pile and shear wave velocity of the soil. For the linear case, results of both real and imaginary parts can be verified with those obtained by the frequency domain solutions. It can be observed that there is not much variation in real part (stiffness) with frequency while imaginary part

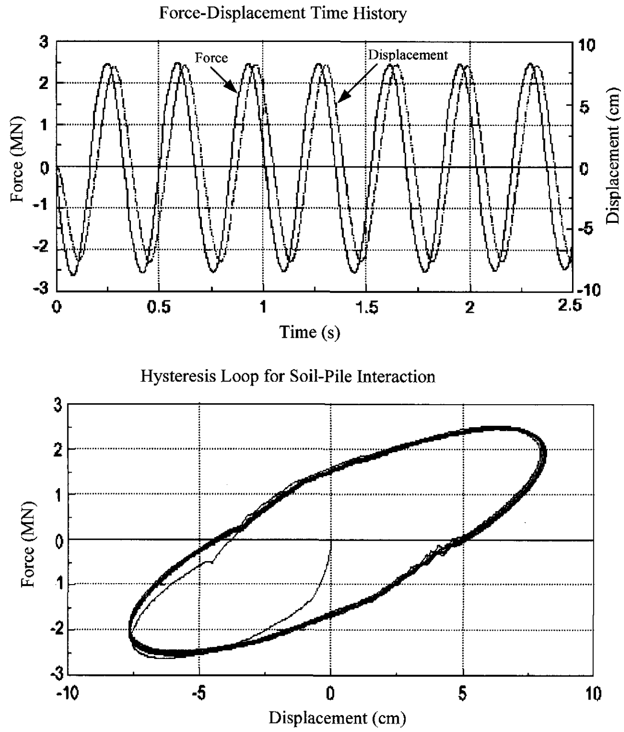

Fig. 13. Behavior of soil-pile interaction in top layer assuming separation at one face (with phase correction)

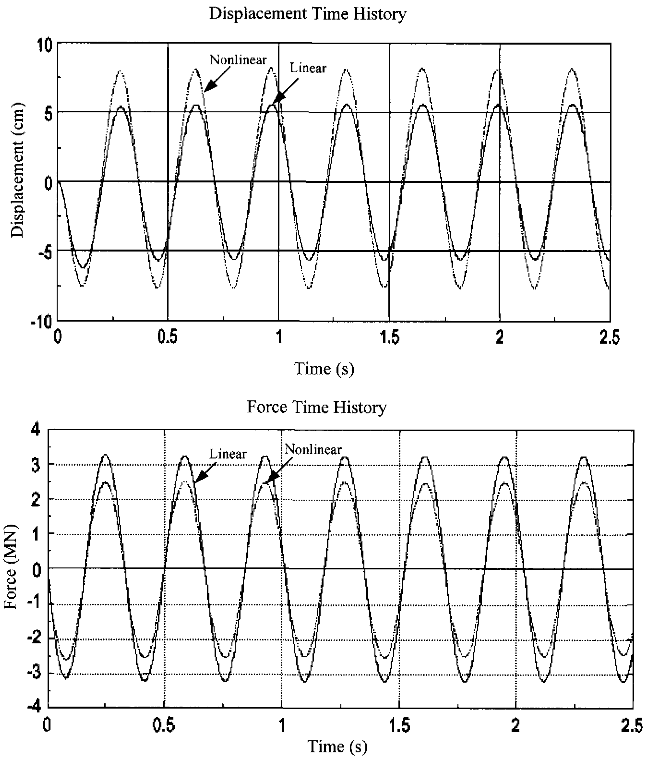

Fig. 14. Comparison of linear and nonlinear response of a single pile

(damping) is almost linearly increasing with frequency. Trends of the results are similar to those shown by Kaynia and Kausel (1982) and Maheshwari and Watanabe (1998). This verifies the proposed method again.

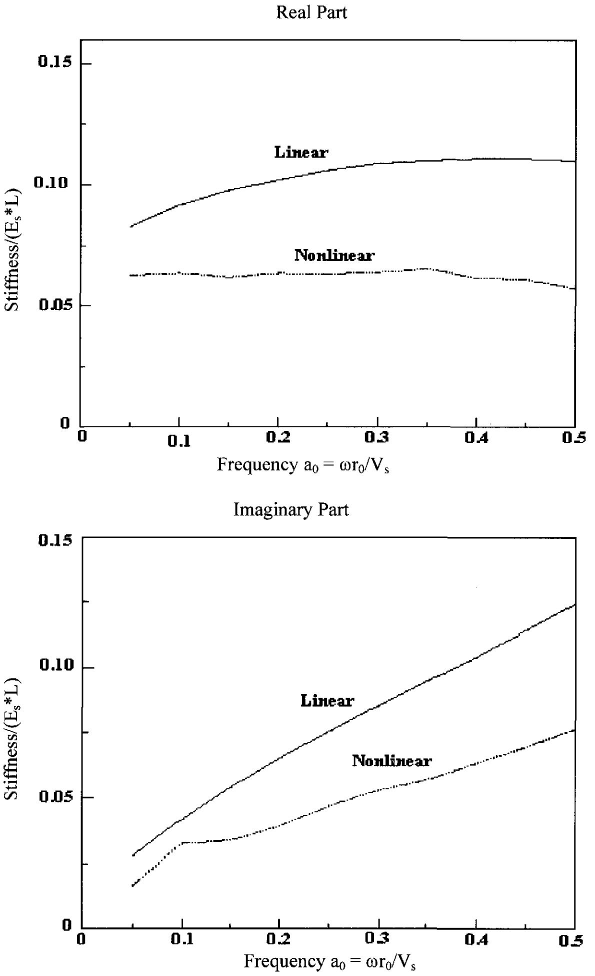

Fig. 15. Linear and nonlinear pile head stiffness with frequency

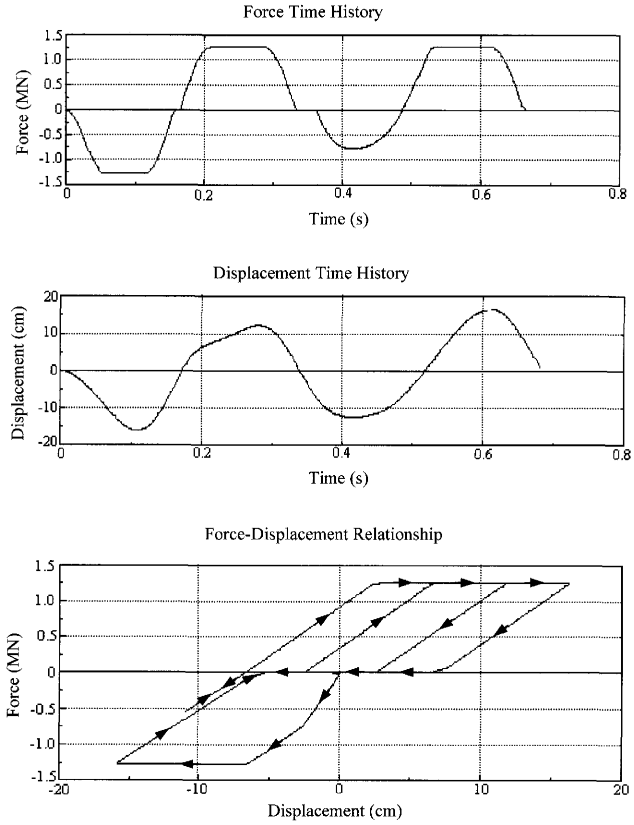

Fig. 16. Behavior of soil-pile interaction in top layer assuming separation on both faces, without damping for ($R=0.3$)

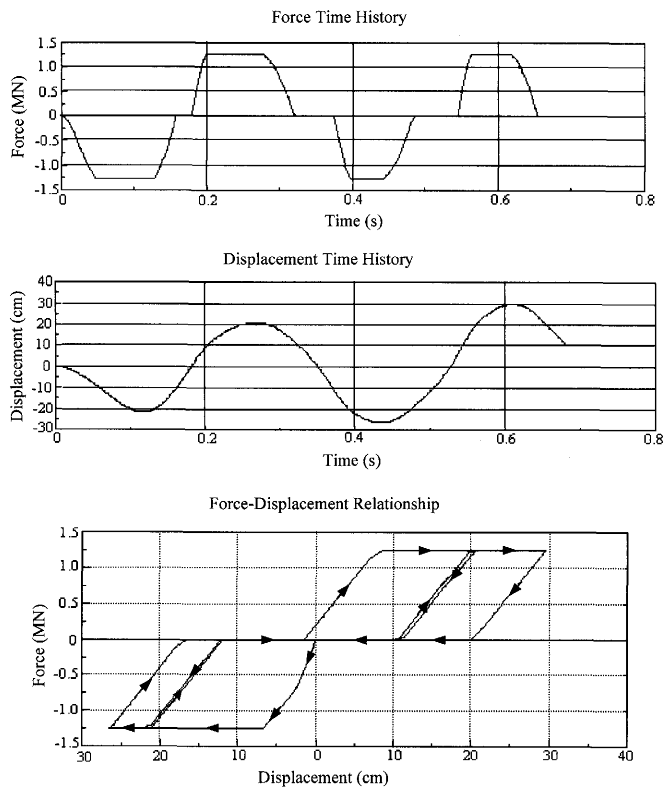

Fig. 17. Behavior of soil-pile interaction in top layer assuming separation on both faces, without damping for ($R=0.35$)

Also it can be observed in Fig. 15 that due to nonlinearity both the real and imaginary parts of the stiffness are decreasing at all frequencies of excitation. Also effect of nonlinearity is much sensitive to frequency of excitation. In general, for the data used in the analysis, effect was more at higher frequencies and relatively less at low frequencies (around $a_0=0.1$). Thus the difference between linear and nonlinear stiffness is increasing with frequency of excitation.

The results presented in Figs. 14 and 15 have similar trends as those presented by Nogami et al. (1992) for separation at the soil-pile interface thus validating presented approach. Also similar effects of separation were observed by Maheshwari et al. (2003) for a single pile and Maheshwari et al. (2004) for pile group using a three-dimensional finite element model.

Separation on Both Faces

Further results are derived for separation on both faces, i.e. when a gap is formed. Figures 16 and 17 show these results for two cycles of loading when there is no damping in the soil media for two different levels of nonlinearity. Level of nonlinearity is defined by a factor R given by

$$R = P_{\max}/(p_c \times L) \quad (17)$$

where $P_{\max}$ is the amplitude of the force for harmonic excitation, while p_c is defined in Eq. (10).

From Figs. 16–17, it can be observed that as time elapses, the amplitude of the displacement in both cases increases, while the force remain limited due to yielding. Duration for which force becomes zero (in Force-Time history—top figure) corresponds to delinking. Comparison of Figs. 16 and 17 reveals that when the amplitude of the excitation is increased (i.e. value of R is increased from 0.3 to 0.35) the amount of gap between soil and pile increases significantly. Also displacement is increased significantly and hysteresis loop becomes wider.

CONCLUSIONS

A new approach is presented to perform the analysis for separation (at the soil-pile interface), using the existing time domain Winkler soil model. Material nonlinearity of soil is also accounted in the analysis. For different possible cases of separation, skeleton curves are shown and the constitutive relationships are formulated. Also relevant formulation is developed. For dealing with separation, a phase correction is necessary. A method to estimate this correction is proposed.

It was observed that response of pile foundation increases significantly due to geometrical nonlinearity (separation). The dynamic stiffness of the soil-pile system decreases considerably. The effect of separation on the response and the dynamic stiffness is frequency dependent and increases with the level of nonlinearity. As the level of nonlinearity increases, separation becomes more intense, heading towards yielding and delinking and thus increasing the gap. Though the results derived in this paper are for a single pile but the proposed methodology can readily be extended for pile groups.

As the effect of separation on the response of pile foundations was significant, the proposed method assumes practical importance in the rational and safe design of pile foundations for earthquake loading.

ACKNOWLEDGEMENT

The research work presented here was performed at the Dept. of Civil Engineering, Saitama University, Japan and supported by Monbusho fellowship for doctoral research by the Ministry of Education, Science, and Culture, Government of Japan. This support is gratefully acknowledged.

REFERENCES

1) Angelides, D. and Roesset, J. M. (1981): Nonlinear lateral dynamic stiffness of piles, *J. Geotech. Engrg. Div.*, ASCE, **107**(11), 1443–1460.
2) Blaney, G. W., Kausel, E. and Rosset, J. M. (1976): Dynamic stiffness of piles, *Proc. 2nd Int. Conf. Num. Meth. Geomech.*, Blacksburg, Virginia, **2**, 1001–1012.
3) Dobry, R. and Gazetas, G. (1988): Simple method for dynamic stiffness and damping of floating pile groups, *Geotechnique*, **38**, 557–574.
4) El Naggar, M. H. and Novak, M. (1996): Nonlinear analysis for dynamic lateral pile response, *Soil Dynamics and Earthquake Engineering*, **15**, 233–244.
5) Gazetas, G. (1984): Seismic response of end-bearing single piles, *Soil Dynamics and Earthquake Engineering*, **3**(2), 82–93.
6) Hardin, B. O. and Drnevich, V. P. (1972): Shear modulus and damping in soils: design equations and curves, *J. Soil Mech. Found. Div.*, ASCE, **98**(7), 667–692.
7) Ishihara, K. (1996): *Soil Behavior in Earthquake Geotechnics*, Clarendon Press, Oxford.
8) Kaynia, A. M. and Kausel, E. (1982): Dynamic behavior of pile groups, *Proc. 2nd Int. Conf. Num. Meth. in Offshore Piling*, Austin, Texas, 509–532.
9) Maheshwari, B. K. (1997): Soil-structure interaction on the structures with pile foundation: three-dimensional nonlinear dynamic analysis of pile foundation, *Ph.D. Dissertation*, Dept. of Civil Engineering, Saitama University, Japan.
10) Maheshwari, B. K. and Watanabe, H. (1998): Nonlinear seismic analysis of pile foundation, *Proc. 11th Eur. Conf. Earthq. Engrg.*, Paris, CD-ROM Paper No. 283.
11) Maheshwari, B. K., Truman, K. Z. and El Naggar, M. H. (2003): Nonlinear time domain analysis of single piles by FEM, *Indian Geotech. J.*, **33**(4), 347–374.
12) Maheshwari, B. K., Truman, K. Z., El Naggar, M. H. and Gould, P. L. (2004): Three-dimensional finite element nonlinear dynamic analysis of pile groups for lateral transient and seismic excitations, *Can. Geotech. J.*, **41**, 118–133.
13) Makris, N. and Gazetas, G. (1992): Dynamic pile-soil-pile interaction, part II: lateral and seismic response, *Earthquake Engineering and Structural Dynamics*, **21**, 145–162.
14) Matlock, H., Foo, S. H. C. and Bryant, L. M. (1978): Simulation of lateral pile behavior under earthquake motion, *ASCE Specialty Conf. Earthquake Engineering and Soil Dynamics*, Pasadena, California, 600–619.
15) Nogami, T. and Konagai, K. (1986): Time domain axial response of dynamically loaded single piles, *J. Engrg. Mech. Div.*, ASCE, **112**(11), 1241–1252.
16) Nogami, T. and Konagai, K. (1987): Dynamic response of vertically loaded nonlinear pile foundation, *J. Geotech. Engrg. Div.*, ASCE, **113**(2), 147–160.
17) Nogami, T. and Konagai, K. (1988): Time-domain flexural response of dynamically loaded single piles, *J. Engrg Mech. Div.*, ASCE, **114**(9), 1512–1525.
18) Nogami, T., Otani, J., Konagai, K. and Chen, H. L. (1992): Nonlinear soil-pile interaction model for dynamic lateral motion, *J. Geotech. Engrg. Div.*, ASCE, **118**(1), 89–106.
19) Novak, M. (1974): Dynamic stiffness and damping of piles, *Can. Geotech. J.*, **11**(4), 574–598.
20) Novak, M. and Nogami, T. (1977): Soil-pile-interaction in horizontal vibration, *Earthquake Engineering and Structural Dynamics*, **5**, 263–281.
21) Novak, M., Nogami, T. and Aboul-Ella, F. (1978): Dynamic soil reaction for plane strain case, Technical note, *J. Engrg. Mech. Div.*, ASCE, **104**(4), 953–956.
22) Watanabe, H. (1978): A consideration on equivalent linearization method of stress-strain hysteresis of soils under cyclic loading, *Report No. E 377007*, Central Research Institute of Electric Power Industry, Japan.
23) Wolf, J. P. (1985): *Dynamic Soil-Structure Interaction*, Prentice-Hall, Inc., Englewood Cliffs, New Jersey.